This document was prepared in conjunction with work accomplished under Contract No. DE-AC09-96SR18500 with the U. S. Department of Energy.

Proceeding of PVP2005
2005 ASME Pressure Vessels and Piping Division Conference
July 17-21, 2005, Denver, Colorado USA

PVP2005-71538

STRESS AND SEALING PERFORMANCE ANALYSIS OF CONTAINMENT VESSEL

Tsu-te Wu

Savannah River National Laboratory
Aiken, South Carolina 29808
(803) 725-8201, tsu-te.wu@srnl.doe.gov

ABSTRACT

This paper presents a numerical technique for analyzing the containment vessel subjected to the combined loading of closure-bolt torque and internal pressure. The detailed stress distributions in the O-rings generated by both the torque load and the internal pressure can be evaluated by using this method. Consequently, the sealing performance of the O-rings can be determined.

The material of the O-rings can be represented by any available constitutive equation for hyperelastic material. In the numerical calculation of this paper, the form of the Mooney-Rivlin strain energy potential is used.

The technique treats both the preloading process of bolt tightening and the application of internal pressure as slow dynamic loads. Consequently, the problem can be evaluated using explicit numerical integration scheme.

INTRODUCTION

In the conventional method for the stress analysis of a pressure vessel with bolted closure, the bolt-preload is either neglected or treated as an equivalent linear elastic thermal load. As a result, the sealing performance of the O-rings can not be adequately evaluated.

This paper presents a numerical technique for analyzing the containment vessel subjected to the combined loading of closure-bolt torque and internal pressure. The detailed stress distributions in the O-rings generated by both the torque load and the internal pressure can be evaluated by using this method. Thus, the sealing performance of the O-rings can be determined.

The material of the O-rings can be represented by any available constitutive equation for hyperelastic material. In the numerical calculation of this paper, the form of the Mooney-Rivlin strain energy potential is used (Reference 1).

The technique treats both the preloading process of bolt tightening and the application of internal pressure as slow dynamic loads. Consequently, the problem can be treated as quasi-static.

ANALYSIS

The present analysis simulates the process of closure bolt tightening and the application of the internal pressure. The analysis consists of three load steps. The first load step simulates closure bolt tightening. During the second load step, the bolt torque load is removed while the residue stresses caused by bolt tightening are maintained. The third load step simulates the application of the internal pressure.

Finite-Element Model

Figure 1 shows the containment vessel. The closure head is fastened to the vessel flange by 20 bolts evenly distributed along the circumference. The basic geometry and dimensions of the containment vessel are shown in Figure 2. By considering the axially symmetric configuration of the vessel, only an 18-

degree sector of the vessel is needed to be simulated as long as the boundary conditions reflect the appropriate boundary conditions.

The finite-element model of the containment vessel body consists of 3-D solid elements available in the ABAQUS finite-element computer code as Type C3D8R and Type C3D6 (Reference 1). The O-rings and closure bolts are modeled using the 3-D solid elements (Type C3D8R). The washers are represented by the 3D rigid elements (R3D4). The application of the bolt loads are simulated using the 3D connector elements (Type CONN3D2). Figure 3 shows the finite-element model for the 18-degree section of the containment vessel.

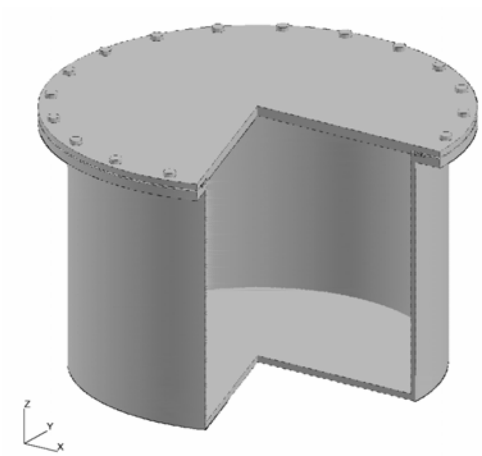

Figure 1. Configuration of Containment Vessel

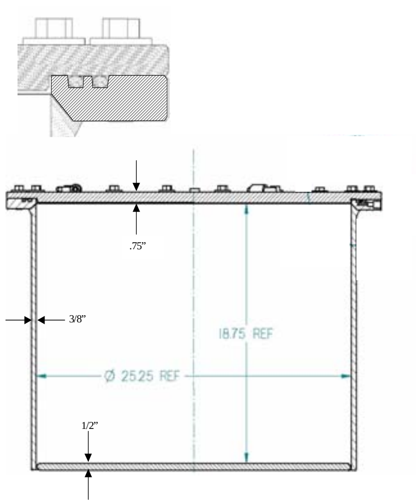

Figure 2. Dimensions of Containment Vessel

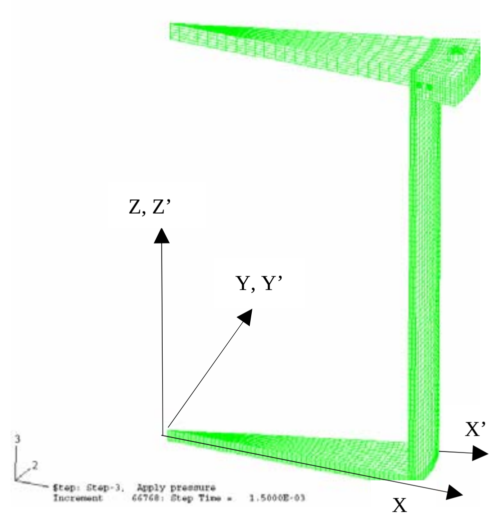

Figure 3. Finite-Element Model

The complex contact conditions between the O-rings and the grooves and between the flange surfaces are monitored by using the general contact options available in the ABAQUS finite-element code.

Boundary Conditions

To enforce the axially symmetric behavior of the containment vessel with respect to the geometric configuration and applied loads, the following boundary conditions are specified.

$UY = 0$ for the nodes on the ZX plane

$UY' = 0$ for the nodes on the $Z'X'$ plane

$UX = 0$ for the nodes along the Z axis

where UX and UY are the displacements in the global x and y axes; UY' is the displacement in the local y' axis. The global and local coordinate systems are defined as in Figure 3.

Contact Conditions

The contact conditions on the interfaces of the model components are simulated using the method of general contact available in the ABAQUS computer code (Reference 1).

Material Properties

The material of the containment vessel including the closure bolt is stainless steel 304L. The stress-strain curve used in the analysis is documented in Reference 2.

The following material constants of the Mooney-Rivlin model for the rubber O-ring are obtained from Reference 3.

$$C_{10} = 464.118 \text{ psi}; \quad C_{01} = 116.03 \text{ psi}$$

The material constant of D_1 is defined by assuming that the ratio of the initial bulk modulus to the initial shear modulus equal to 20, corresponding to Poisson's ratio of 0.475.

Application of Closure Torque Load
The first load step of the analysis is to simulate the application of the closure torque. The torque load applied to each closure bolt generates a tensile load in the bolt. This tensile load in each bolt is simulated using a connector element between the bolt head and the washer.

In the present analysis, the functions of the bolt head and the washer are only to transmit the loads and displacements and the detailed stress distributions in these components are not of interest. Therefore, they are assumed to be rigid and each has its own reference node as illustrated in Figure 4. The tensile load of 3394 pounds is applied instantly at the connect element to pull the reference nodes apart so that the washer compresses the vessel lid while the bolt head is pulling the bolt.

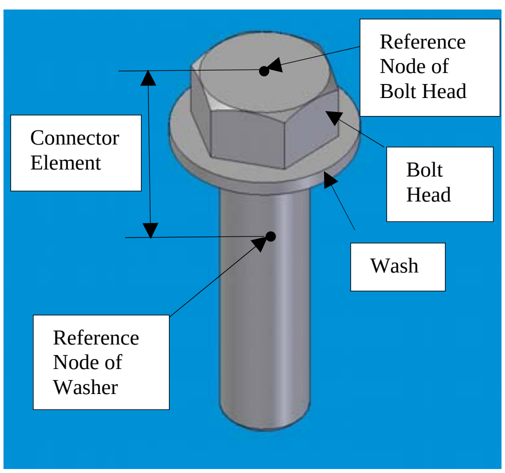

Figure 4. Finite-Element Model of Connect Element

Figure 5 displays the displacement time history of the bolt head with respect to the washer during the duration of the torque load application. The maximum value of this relative displacement caused by the bolt tensile load of 3394 pounds is 0.0934 inches.

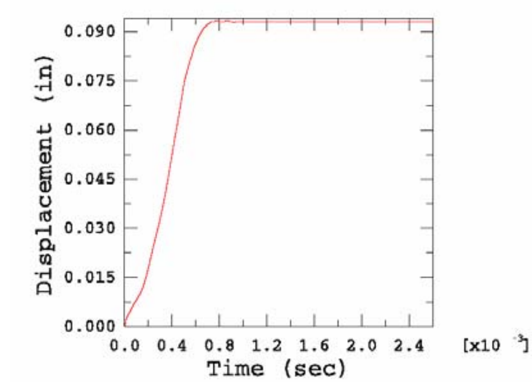

Figure 5. Time-History of Bolt Head/Washer Relative Displacement

Removal of Closure Torque Load

In the second load step (during the duration from 0.001 to 0.0011 seconds), the tensile force in the connector element between the bolt head and the washer is removed. However, the stresses in the vessel containment generated by the torque load in the first load step need to be maintained. This can be accomplished by specifying the connector element motion as a boundary condition to keep the bolt head and the washer apart at the constant distance of 0.0934 inches. The value of 0.0934 inches has been determined in the first load step and is shown in Figure 5.

Application of Internal Pressure
The third load step is to simulate the application of the internal pressure. The distributed load of 20 psi is applied as a step load on the inner surface of the containment vessel. In addition, the stresses caused by the bolt torque load are maintained using the same technique discussed above.

DISCUSSION OF RESULTS

<u>Time-History of Energy Components</u>
Figure 6 shows the combined time history of the energy components for the three load steps. Since the kinetic energy at the end of the final load step is small compared to the internal energy, the effect of the inertial force introduced by the dynamic loading process on the final results is negligible. Therefore, the dynamic approach to the evaluation of O-ring sealing performance in the containment vessel is valid.

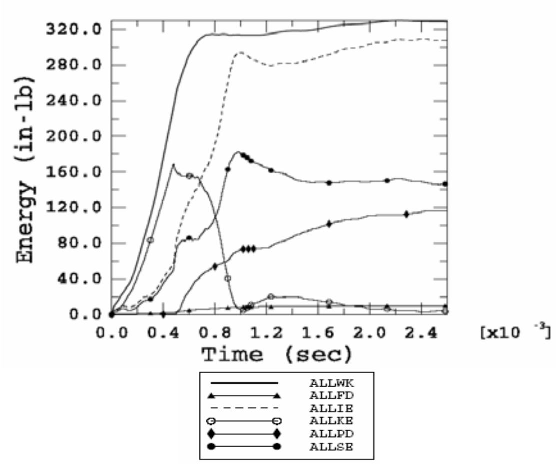

allwk = external work; allfd = friction dissipation energy;
allie = internal energy; allke = kinetic energy;
allpd = plastic strain energy; allse =elastic strain energy

Figure 6. Time History of Energy Components

<u>Deformation and Stresses in O-rings</u>

Figure 7 shows the deformed cross sections of the O-rings in the groove when the containment vessel is subjected to the stresses caused by the bolt torque and the internal pressure of 20 psi. The blow-up view of the deformed versus undeformed shapes of the O-rings under the same loading is given in Figure 8. The deformations highlighted in these figures clearly indicated that the containment vessel is effectively sealed.

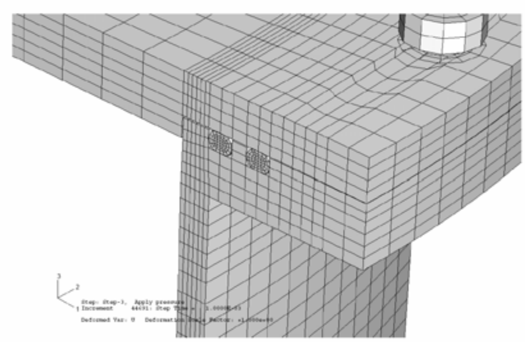

Figure 7. Deformed Cross Sections of O-rings

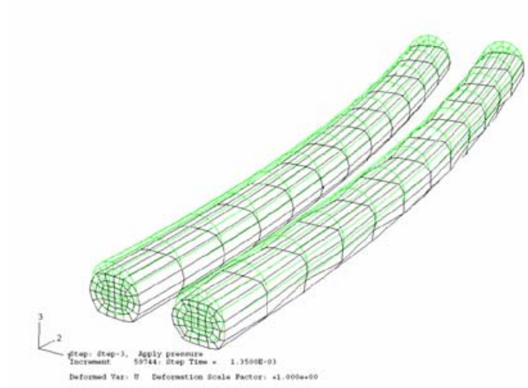

Figure 8. Deformed versus Undeformed Shape of O-rings

<u>Stress Distributions in Containment Vessel</u>

Figure 9 displays the stress distribution in the containment vessel for the bolt tensile force of 3394 pounds caused by the closure bolt torque load. The stress distribution in the containment vessel caused by the internal pressure of 20 psi together with the stresses due to the closure torque load is shown in Figure 10.

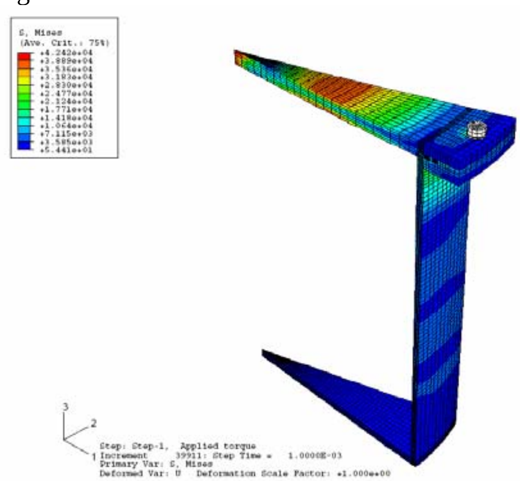

Figure 9. Stress Distribution for Closure Torque Load

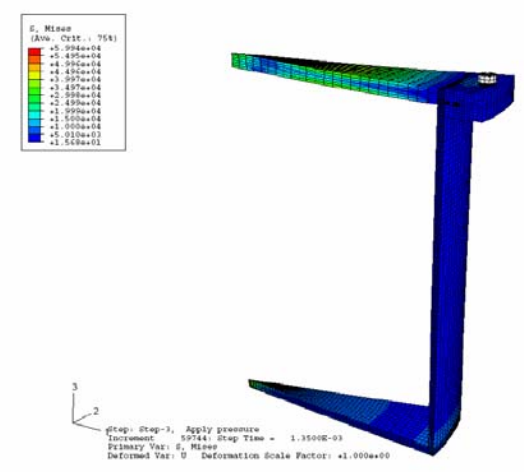

Figure 10. Stress Distribution for Internal Pressure and Torque Load Residue Stresses

CONCLUSION

A numerical technique has been developed to analyze the containment vessel subjected to the combined loading of closure-bolt torque and internal pressure. The technique treats both the preloading process of closure bolt tightening and the application of the internal pressure as dynamic loads. The problem can thus be solved using the explicit numerical integration scheme, which is more suitable for complex contact conditions. As long as the duration of the loading process is long enough, the inertia effects on the analytical results are negligible.

REFERENCES

1. ABAQUS User's Manual – Analysis, Version 6.4, ABAQUS, Inc. 2003.

2. Wu, T. T., Blanton, P. S., and Smith, A. C., "Dynamic Analysis of 9975 Shipping Package without Overpack Subjected to 55-Foot Drop," PVP-VOL 425, 2001.

3. Getting Started with ABAQUS, Version 6.4, ABAQUS, Inc. 2003.